ARTICLE

https://doi.org/10.1038/s41586-018-0673-2

Anthropogenic influences on major tropical cyclone events

Christina M. Patricola[1]* & Michael F. Wehner[2]

There is no consensus on whether climate change has yet affected the statistics of tropical cyclones, owing to their large natural variability and the limited period of consistent observations. In addition, projections of future tropical cyclone activity are uncertain, because they often rely on coarse-resolution climate models that parameterize convection and hence have difficulty in directly representing tropical cyclones. Here we used convection-permitting regional climate model simulations to investigate whether and how recent destructive tropical cyclones would change if these events had occurred in pre-industrial and in future climates. We found that, relative to pre-industrial conditions, climate change so far has enhanced the average and extreme rainfall of hurricanes Katrina, Irma and Maria, but did not change tropical cyclone wind-speed intensity. In addition, future anthropogenic warming would robustly increase the wind speed and rainfall of 11 of 13 intense tropical cyclones (of 15 events sampled globally). Additional regional climate model simulations suggest that convective parameterization introduces minimal uncertainty into the sign of projected changes in tropical cyclone intensity and rainfall, which allows us to have confidence in projections from global models with parameterized convection and resolution fine enough to include tropical cyclones.

Tropical cyclones are among the deadliest and most destructive natural disasters. Hurricane Katrina was the costliest natural disaster in the USA, causing at least 1,833 deaths and costing US$160 billion in damages (all dollars adjusted to 2017) along the Gulf Coast of the USA in August 2005[1]. A close second is hurricane Harvey, which stalled over the Houston metropolitan area in August 2017, causing record flooding. Hurricane Harvey was followed in September by hurricane Irma, which heavily affected the Virgin Islands and Florida Keys, and hurricane Maria, which caused lasting devastation in Puerto Rico. In total, the hyperactive 2017 Atlantic hurricane season caused at least US$265 billion in damages and 251 fatalities, probably a staggering underestimate owing to crippled communications and infrastructure in Puerto Rico, which meant that many hurricane-related deaths were unconfirmed. To improve the resiliency of coastal and island communities, it is critical to understand the drivers of tropical cyclone variability and change. However, the response of tropical cyclone activity to climate change, so far and in the future, remains uncertain[2–4].

There is no consensus regarding whether climate change until now has influenced tropical cyclone activity, given that natural variability is large and tropical cyclone observation methodologies have changed over time. As yet, there has been no detectable trend in tropical cyclone frequency. Although a positive trend in Atlantic tropical cyclone number has been observed since 1900, it is due primarily to increases in short-lived tropical cyclones, which were probably undersampled during the pre-satellite era when observations over ocean were taken by ship[5]. Subjective measurements and variable observation procedures pose serious challenges to detecting trends in tropical cyclones[6]. This is apparent even when observations are adjusted in attempt to normalize for changing sampling procedures over time, owing to large natural variability[7]. In addition, it remains inconclusive whether there have yet been trends in global tropical cyclone intensity, with increases detected in some basins[8–11]. The strong influences on tropical cyclones of multi-decadal variability including the Atlantic Multidecadal Oscillation[12,13] and interannual variability including the El Niño–Southern Oscillation and Atlantic Meridional Mode[14–17] make disentangling the influences of climate variability and change on trends in tropical cyclone activity all the more challenging.

Looking into the future, there is no consensus regarding how anthropogenic emissions are expected to change global tropical cyclone frequency, with the majority of climate models projecting fewer tropical cyclones[18–22] but others more tropical cyclones[23] (see also references within refs [2–4]). However, maximum potential intensity theory and recent climate modelling studies suggest increases in the future number of intense tropical cyclones[21,22,24–29]. In addition, climate model simulations suggest that rainfall associated with tropical cyclones will increase in future warmer climates, but with large uncertainty in magnitude[18,20,28,30–33]. The Clausius–Clapeyron relation dictates that the saturation specific humidity of the atmosphere increases by 7% per 1 °C of warming, providing a constraint on changes in moisture available for precipitation. If tropical cyclone precipitation efficiency does not change, then changes in precipitation follow Clausius–Clapeyron scaling as the oceans warm[34]. However, recent studies of hurricane Harvey found 15%–38% increases in storm total precipitation attributable to global warming, well above the Clausius–Clapeyron limit of 7% given anthropogenic warming of 1 °C in the Gulf of Mexico[35–37]. Such rainfall over Houston—a once-every-2,000-year event in the late twentieth century—is expected to become a more common one-per-century event by the end of the twenty-first century[38].

There is no theory of tropical cyclone formation to predict how tropical cyclones are expected to change in the future, and the problem is complicated by potentially compensating influences of greenhouse gases. Although the factors that influence tropical cyclones are well understood, with favourable conditions including a warm upper-ocean temperature, an unstable atmosphere with a moist mid-troposphere, and weak vertical wind shear[39], the way in which these factors will change, and which ones will dominate, is unknown. Sea-surface temperature (SST) warming has been observed and is expected to continue, which would intensify tropical cyclones[8]. However, sub-surface ocean

[1]Climate and Ecosystem Sciences Division, Lawrence Berkeley National Laboratory, Berkeley, CA, USA. [2]Computational Research Division, Lawrence Berkeley National Laboratory, Berkeley, CA, USA. *e-mail: cmpatricola@lbl.gov

Table 1 | Tropical cyclone peak 10-m wind speed

Basin	Tropical cyclone	Resolution	Historical minus pre-industrial	RCP4.5 minus historical	RCP6.0 minus historical	RCP8.5 minus historical	Historical	Observed
Atlantic	Katrina	27 km (P)	−1.0			11.0**	101	150
		9 km (P)	2.0			15.2**	123	150
		9 km	−0.5			13.5**	127	150
		3 km	−2.4			13.7**	149	150
		4.5 km		6.0**	8.5**	13.8**	142	150
	Irma	4.5 km	−1.9	7.3**	10.4**	12.4**	143	160
	Maria	4.5 km	−1.5	7.5**	10.9**	12.9**	132	150
	Andrew	4.5 km		−3.3	−2.4	−1.7	118	150
	Bob	4.5 km		−6.1**	−2.4*	2.1	78	100
	Floyd	4.5 km		11.2**	13.5**	X	118	135
	Gilbert	4.5 km		18.0**	18.6**	28.8**	109	160
	Ike	4.5 km		12.8**	14.1**	18.0**	127	125
	Matthew	4.5 km		10.6**	11.1**	15.8**	123	145
Eastern Pacific	Iniki	4.5 km		−0.4	−3.9	4.6*	114	125
Northwest Pacific	Haiyan	4.5 km		6.7**	3.8	12.3**	124	170
	Morakot	4.5 km		0.5	X	X	71	80
	Songda	4.5 km		10.4**	5.5**	X	109	125
South Pacific	Yasi	4.5 km		11.2**	13.7**	18.9**	95	135
Southwest Indian	Gafilo	4.5 km		8.6**	8.8**	16.8**	110	140

The ensemble-mean difference in tropical cyclone peak 10-m wind speed is given (in knots) between the historical and pre-industrial simulations and between the RCP4.5, RCP6.0 and RCP8.5 simulations and the historical simulation, along with the tropical cyclone peak 10-m wind speed from observations and the ensemble-mean historical simulation. Cases of substantial differences between simulated and observed tropical cyclone tracks are denoted X (see Methods) and simulations that were not performed are blank. *Changes significant at the 10% level; **changes significant at the 5% level. Simulations that used convective parameterization are denoted 'P'.

structure changes are also important for tropical cyclone intensity, and may be a dampening effect in the future[40]. Considering atmospheric factors, anthropogenic warming is expected to be greater in the upper compared to lower troposphere in response to increased greenhouse gases, which could weaken tropical cyclones. However, the tropical tropopause is expected to cool as its height increases, which would strengthen the maximum potential intensity of tropical cyclones, as observed in the Atlantic[41,42]. Because maximum potential intensity theory applies to mature tropical cyclones, this means the strength of intense tropical cyclones may increase. In addition to thermodynamic influences on tropical cyclones, changes in atmospheric circulation are also important. Projected increases in vertical wind shear could work to suppress tropical cyclones regionally[43]. Finally, it is uncertain how the seedling disturbances that serve as tropical cyclone precursors may change.

Observational consistency issues and compensating physical mechanisms for tropical cyclone changes are only some of the challenges in understanding anthropogenic influences on tropical cyclones. In addition, it can be difficult for climate models to represent the observed climatology of intense tropical cyclones, even at the 0.25° horizontal resolution that is considered to be high resolution for global models[21]. Furthermore, the decades-long simulations used to project future tropical cyclone activity typically parameterize convection. However, the associated uncertainty introduced into tropical cyclone projections has not been systematically understood.

The purpose of this study is to advance our understanding of anthropogenic influences on tropical cyclones by quantifying the impact of climate change so far, and in the future, on the intensity and rainfall of destructive tropical cyclone events using convection-permitting regional climate model simulations. We first addressed the question of how tropical cyclone intensity and rainfall could change if hurricanes like Katrina, Irma and Maria occurred in pre-industrial or future warmer climates. We then investigated the robustness of our results by extending the analysis to 15 tropical cyclone events sampled globally under three future climates. Finally, we quantified the uncertainty in these estimates associated with convective parameterization for hurricane Katrina.

Convection-permitting tropical cyclone simulations

We performed simulations with the Weather Research and Forecasting (WRF) regional climate model, which is developed by the National Center for Atmospheric Research (NCAR). Control simulations for each tropical cyclone event consist of ten-member ensemble hindcasts representing the historical conditions in which the tropical cyclone actually occurred, with boundary conditions from reanalysis or observations (Methods). We also performed experiments representing hurricanes Katrina, Irma and Maria if they were to occur in a pre-industrial climate, as well as 15 tropical cyclone events sampled globally at the end of the twenty-first century under the Representative Concentration Pathways emissions scenarios RCP4.5, RCP6.0 and RCP8.5 (listed in Table 1). Although previous studies considered individual tropical cyclones, the modelling frameworks used differ (Methods). Our use of one model for many events allows us to assess the robustness of the climate change responses more directly among events. We selected tropical cyclones that were particularly destructive (in terms of fatalities and economic losses) and represent various tropical cyclone basins. Many of the tropical cyclones were intense in terms of wind speed, but two were weak tropical cyclones with moderate-to-heavy rainfall (typhoon Morakot and hurricane Bob). Boundary conditions for the pre-industrial and Representative Concentration Pathway experiments were based on those from the historical, adjusted to remove and add, respectively, the thermodynamic component of climate change (Methods). Simulations of all tropical cyclones were performed at a convection-permitting horizontal resolution of 4.5 km. To investigate uncertainty in the response of tropical cyclones to anthropogenic forcings caused by convective parameterization, we performed additional simulations of hurricane Katrina at horizontal resolutions of 3 km, 9 km (both without and with parameterization) and 27 km.

Anthropogenic influences on tropical cyclone intensity

To evaluate anthropogenic influences on hurricanes Katrina, Irma and Maria, we first verified that the hindcasted tropical cyclone tracks reasonably represent the observed tracks. Indeed, this is the case for each ensemble member of the historical simulations, as well as the ensemble

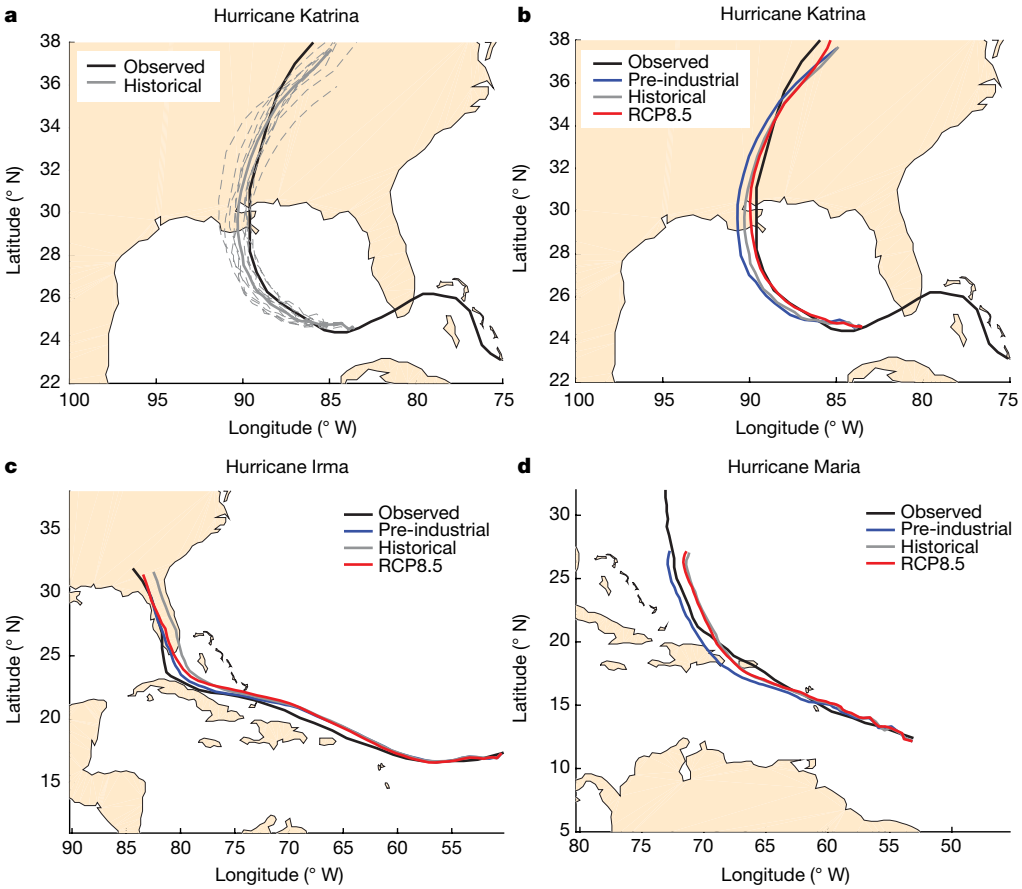

Fig. 1 | Tropical cyclone tracks. a, **b**, Hurricane Katrina's observed track (black) with simulated tropical cyclone tracks from ten ensemble members (grey dashed line) and the ensemble mean (grey solid line) of the historical simulation (**a**) and the ensemble mean of historical (grey), pre-industrial (blue) and RCP8.5 (red) simulations at 3-km resolution (**b**). **c**, **d**, As in **b**, for hurricanes Irma (**c**) and Maria (**d**) at 4.5-km resolution.

means (Fig. 1 and Extended Data Fig. 1). (We note a bias in hurricane Irma's landfall that is more noticeable owing to Florida's longitudinally narrow geography; also the simulated hurricane Maria slightly missed direct landfall over Puerto Rico.) In addition, the simulated tropical cyclone tracks are robust to anthropogenic perturbations (Fig. 1b–d), indicating that comparisons among experiments are fair (Methods). Next, we estimated the model's ability to simulate the observed intensity of the tropical cyclones, recognizing the challenges of such observation–model comparison (Methods). The time series of maximum 10-m wind speed (Fig. 2a–c) and minimum sea-level pressure (SLP) (Extended Data Fig. 2a–c) show that the hindcasted intensity is close to what was observed for hurricane Katrina, but underestimated for hurricanes Maria and Irma. In addition, a period of rapid intensification was observed for all three hurricanes, which was most pronounced for hurricane Maria. However, the hindcasts failed to represent rapid intensification, a challenge that remains in operational forecasting[44].

Given that the simulated hurricane tracks and intensities compare reasonably well with the observed tracks, albeit with a failure to reproduce rapid intensification, we evaluated the response in hurricane intensity to past and future anthropogenic forcings. For each of the hurricanes, the ensemble-mean wind speed and SLP-based intensity time series are indistinguishable between the pre-industrial and historical simulations, whereas there is a distinct increase in intensity from the historical to RCP8.5 climates for a substantial portion of each hurricane's lifetime (Fig. 2a–c and Extended Data Fig. 2a–c). To assess the significance ($P = 0.05$) of the intensity changes, we calculated the peak intensity over each hurricane's lifetime based on maximum wind speed (Fig. 2d–f) and minimum SLP (Extended Data Fig. 2d–f) for each ensemble member of the pre-industrial, historical and RCP8.5 simulations. We found that climate change at the time of the event weakly and insignificantly ($P = 0.05$) influenced the intensity of hurricanes Katrina, Irma and Maria (Table 1 and Extended Data Fig. 3), corresponding to similar ensemble spreads between the pre-industrial and historical simulations (Fig. 2d–f). On the other hand, hurricanes like Katrina, Irma and Maria are expected to significantly ($P = 0.05$) intensify with continued warming (Table 1 and Extended Data Fig. 3), corresponding to a shift towards greater intensities for the RCP8.5 simulations compared to the historical (Fig. 2d–f).

We extended the investigation to 15 tropical cyclone events sampled globally under three future climate scenarios, to address the robustness of the results. We performed the same analysis for all 15 tropical cyclones as was presented above for hurricanes Katrina, Irma and Maria, including an evaluation of the historical hindcast's ability to reproduce the observed tropical cyclone track. Of the 45 experiments, four were discarded for tropical cyclone tracks that deviated substantially from the historical case (Methods). Of the 15 tropical cyclones, 13 of which were intense, 11 show significant ($P = 0.05$) intensity increases, regardless of emissions scenario, with peak wind speed increases of 6–29 knots and minimum SLP reduced by 5–25 hPa (Table 1 and Extended Data Fig. 3). Changes are insignificant for hurricanes Andrew and Iniki, and hurricane Bob significantly weakens. Therefore, the experiments provide substantial support for strengthening of intense tropical cyclone events globally for the three future climate scenarios considered.

Finally, we quantified the uncertainty in the response of tropical cyclones to anthropogenic forcings owing to convective parameterization using simulations of hurricane Katrina at resolutions of 3 km, 9 km and 27 km. Regardless of resolution, these simulations produced insignificant changes in Katrina's intensity from the pre-industrial to historical climates, and a substantial and significant ($P = 0.05$) increase in intensity from the historical to RCP8.5 climates (Fig. 2d and Table 1), indicating that the qualitative simulated tropical cyclone response to

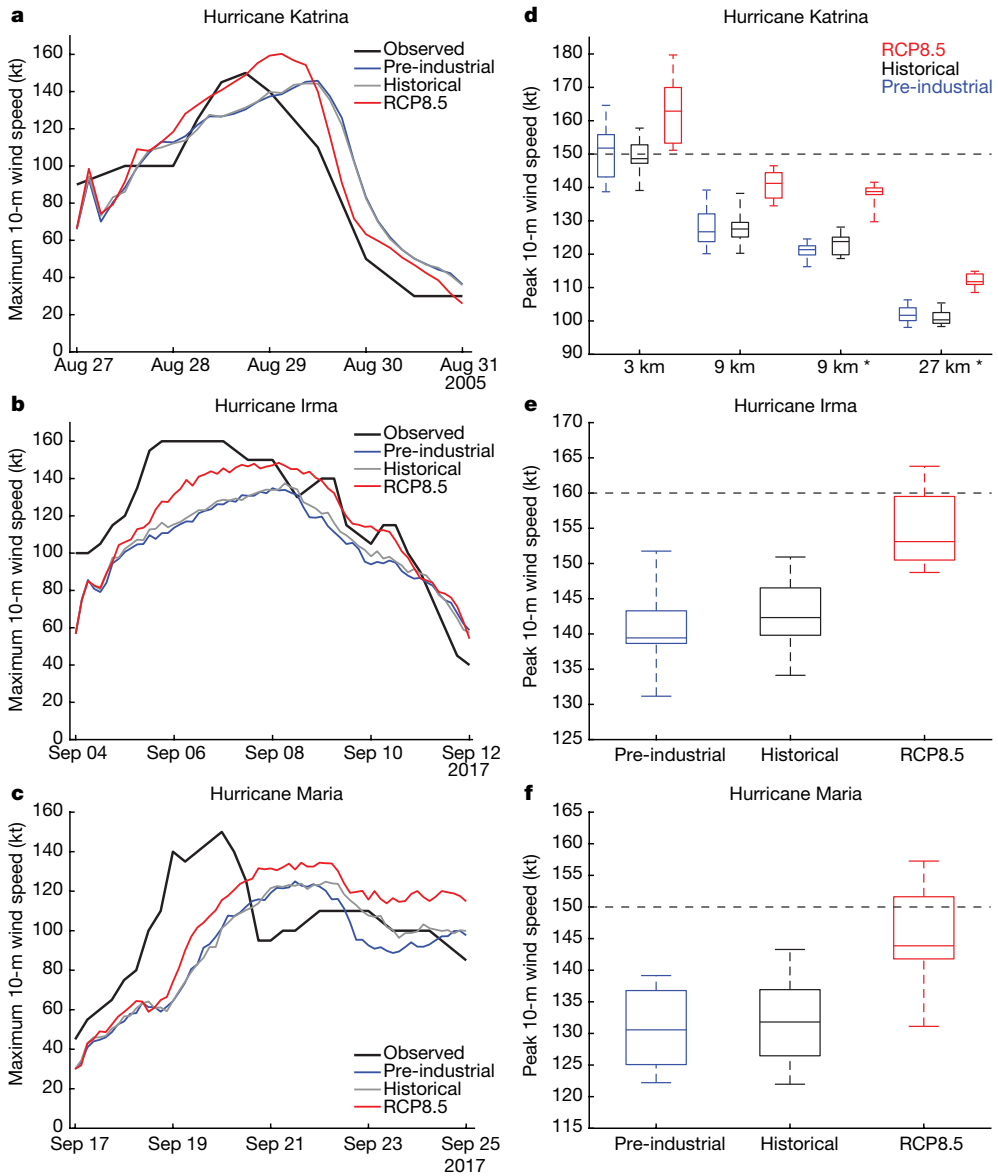

Fig. 2 | Time series and boxplots of tropical cyclone maximum 10-m wind speed. a–c, The time series of maximum 10-m wind speed (knots, kt) from observations (black) and the ensemble mean of the pre-industrial (blue), historical (grey) and RCP8.5 (red) simulations of hurricanes Katrina at 3-km resolution (**a**), Irma at 4.5-km resolution (**b**) and Maria at 4.5-km resolution (**c**). **d–f**, Boxplots of peak 10-m wind speed (kt) from the ten-member ensemble of pre-industrial (blue), historical (black) and RCP8.5 (red) simulations of hurricane Katrina at 3-km, 9-km (with and without convective parameterization) and 27-km resolution (**d**), and of hurricanes Irma (**e**) and Maria (**f**) at 4.5-km resolution. The centre line denotes the median, box limits denote lower and upper quartiles, and whiskers denote the minimum and maximum. The observed peak intensity is marked with a horizontal dashed black line. Simulations that used convective parameterization are denoted by an asterisk.

anthropogenic forcing may be insensitive to use of convective parameterization and model resolution between 3 km and 27 km in this model, with additional work needed to make a generalized conclusion. Furthermore, the range of the future response is relatively small between resolutions, covering a 11–15 knot increase in maximum wind speed and a 11–14 hPa decrease in minimum SLP. However, model resolution substantially affects absolute intensity, as expected, with an ensemble-mean Category 5, Category 4 and Category 3 hurricane produced by the historical simulations at 3-km, 9-km and 27-km resolution, respectively.

Anthropogenic influences on tropical cyclone rainfall

Although tropical cyclone winds can cause substantial damages, heavy rainfall can pose an equal, if not greater, hazard. We analysed anthropogenic changes in rainfall within a reference frame centred on the tropical cyclone, called a 'composite' (Fig. 3), because even small changes in tropical cyclone track and translation speed confound a geographically fixed analysis. The composites include the simulated tropical cyclone lifetime, excluding a generous 12-h spin-up, and cover ocean and land. Two levels of statistical significance ($P = 0.05$ and $P = 0.10$) are presented, as changes in rainfall tend to be noisy compared with wind speed and SLP. We found that climate change at the time of Katrina significantly ($P = 0.10$) enhanced rainfall rates by 4%–9% over an approximately 5° × 5° box centred on the tropical cyclone, a result qualitatively insensitive to model resolution and use of convective parameterization (Table 2). Likewise, climate change at the time of hurricanes Irma and Maria significantly ($P = 0.10$) increased rainfall by 6% and 9%, respectively, but over a roughly 1.5° × 1.5° box centred on the tropical cyclone (Table 2), owing to a concentration of the rainfall enhancements near the tropical cyclone centre (Fig. 3). Therefore, we find evidence that climate change so far has begun to enhance rainfall for these three tropical cyclones, with investigation of additional cases needed before making a general conclusion.

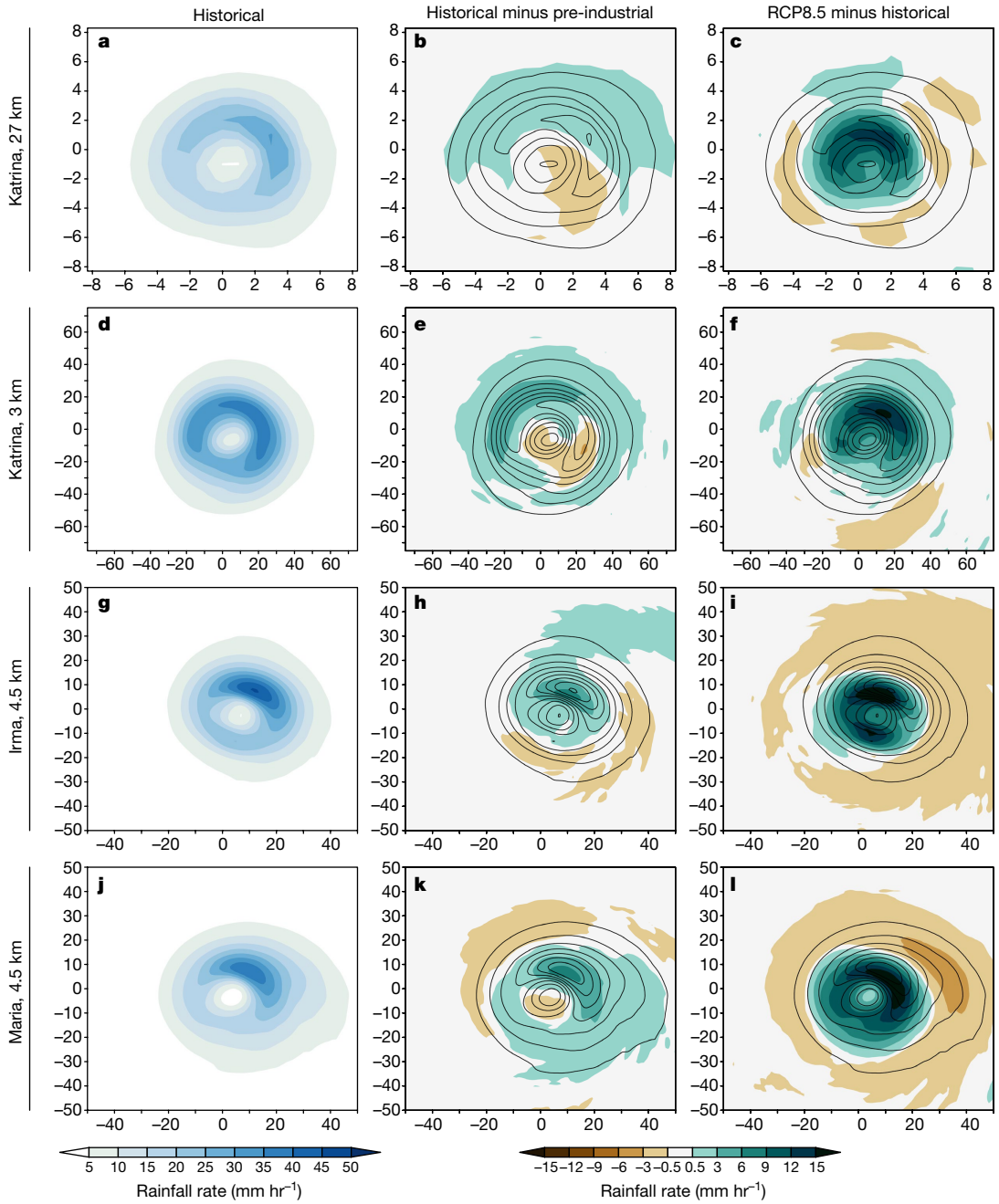

Fig. 3 | Tropical cyclone rainfall composites. a–c, Rainfall rate (colour scale) relative to tropical cyclone centre and throughout the simulated tropical cyclone lifetime from the ensemble mean of the historical (**a**), historical minus pre-industrial (**b**) and RCP8.5 minus historical (**c**) simulations of hurricane Katrina at 27-km resolution. **d–l**, As in **a–c** but for simulations of hurricane Katrina at 3-km resolution (**d–f**) and of hurricanes Irma (**g–i**) and Maria (**j–l**) at 4.5-km resolution. Contours denote the rainfall rate (in millimetres per hour) from the corresponding historical simulation. The *x* and *y* axes show the number of model grid points from the tropical cyclone centre.

In addition, we found robust increases in tropical cyclone rainfall with continued climate change along RCP4.5, RCP6.0 and RCP8.5 scenarios, which are significant for at least one Representative Concentration Pathway scenario for all 15 tropical cyclones except two ($P = 0.10$) or three ($P = 0.05$) (Table 2). The largest increases in rainfall tend to occur over the regions of heaviest historical rainfall (Fig. 3 and Extended Data Fig. 4). For some tropical cyclones, including hurricanes Irma and Maria (Fig. 3), there is a coherent spatial pattern in the future rainfall response characterized by drying in the outer-tropical-cyclone radii, resulting in rainfall responses that are stronger over an approximately 1.5° × 1.5° area compared with a 5° × 5° box (Table 2). Such outer-tropical-cyclone drying is not apparent or is weak for most tropical cyclones considered, including hurricanes Katrina, Floyd, Gafilo and Yasi (Fig. 3 and Extended Data Fig. 4). The future rainfall changes reach 25%–30% for some tropical cyclones under an RCP8.5 scenario (Table 2), exceeding what would be expected by Clausius–Clapeyron scaling alone given regional SST warming of about 2.5 °C in these cases.

We next evaluated changes in extreme rainfall, which can be important for localized flooding, by considering the probability density functions of rainfall rates sampled three-hourly and including each model grid point within about 5° × 5° centred on the tropical cyclone for the lifetime of the simulated storm (Fig. 4). The individual ensemble members of the 3-km-resolution hurricane Katrina simulations exhibit probabilities of extremely intense rainfall rates that consistently increase from the pre-industrial, to historical, to RCP8.5 experiments (Fig. 4a). This behaviour is also apparent in the ensemble means for simulations at 3-km and 27-km resolution; however, the coarser-resolution simulation consistently produces weaker extremes (Fig. 4b). The increasing

Table 2 | Changes in tropical cyclone rainfall

Basin	Tropical cyclone	Resolution	(Historical minus pre-industrial)/pre-industrial	(RCP4.5 minus historical)/historical	(RCP6.0 minus historical)/historical	(RCP8.5 minus historical)/historical
Atlantic	Katrina	27 km (P)	4.7**			13.0**
		9 km (P)	4.5*			12.7**
		9 km	5.0*			13.5**
		3 km	8.7**			14.4**
		4.5 km		7.1**	14.6**	16.5**
	Irma	4.5 km	4.2	4.5	8.8**	2.1
	Irma[a]	4.5 km	6.3*	17.5**	26.1**	27.8**
	Maria	4.5 km	4.4	7.0*	7.2*	7.7*
	Maria[a]	4.5 km	8.9**	21.8**	23.4**	36.9**
	Andrew	4.5 km		0.3	5.1	4.8
	Bob	4.5 km		6.5**	11.9**	13.5**
	Floyd	4.5 km		12.3**	13.5**	X
	Gilbert	4.5 km		13.5**	16.5**	25.3**
	Ike	4.5 km		15.0**	20.2**	26.5**
	Matthew	4.5 km		2.0	1.1	4.0
Eastern Pacific	Iniki	4.5 km		5.8*	4.9	15.2**
Northwest Pacific	Haiyan	4.5 km		9.5**	12.8**	31.3**
	Morakot	4.5 km		6.8*	X	X
	Songda	4.5 km		19.5**	10.6**	X
South Pacific	Yasi	4.5 km		15.6**	23.1**	35.2**
Southwest Indian	Gafilo	4.5 km		19.7**	16.8**	41.6**

The ensemble-mean change in rainfall is given (as a percentage) between the historical and pre-industrial simulations and between the RCP4.5, RCP6.0 and RCP8.5 simulations and the historical simulation, averaged over approximately 5° × 5° and over 1.5° × 1.5° (the latter is denoted [a]) boxes centred on the tropical cyclone. Cases of substantial differences between simulated and observed tropical cyclone tracks are denoted X (see Methods) and simulations that were not performed are blank. *Changes significant at the 10% level; **changes significant at the 5% level. Simulations that used convective parameterization are denoted 'P'.

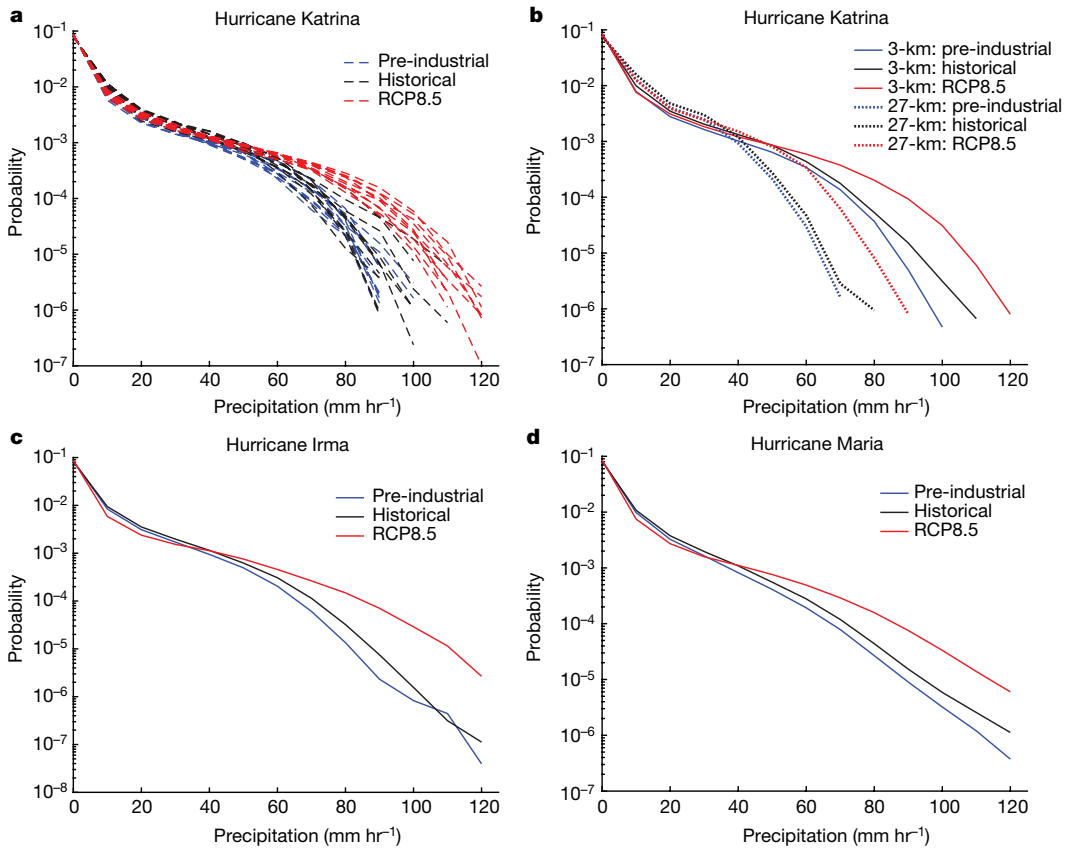

Fig. 4 | Probability density functions of tropical cyclone rainfall rates. **a**–**d**, Probability density functions of rainfall rates from each of ten ensemble members of the pre-industrial (blue), historical (black) and RCP8.5 (red) simulations of hurricane Katrina at 3-km resolution (**a**), and from the ensemble means of simulations of hurricane Katrina at 3-km (solid lines) and 27-km (dotted lines) resolution (**b**) and of hurricanes Irma (**c**) and Maria (**d**) at 4.5-km resolution.

probability of extremely intense rainfall rates with anthropogenic warming is robust among hurricanes Katrina, Irma and Maria (Fig. 4).

Discussion

There is no consensus on whether climate change has yet affected tropical cyclone statistics, and how continued warming may influence many aspects of future tropical cyclone activity. We have improved our understanding of anthropogenic influences on tropical cyclones by quantifying how the intensity and rainfall of historically impactful tropical cyclone events could change if similar events occurred in cooler and warmer climates, using ten-member ensembles of convection-permitting hindcast simulations with boundary conditions adjusted to reflect the different climate states. We found that climate change so far has weakly and insignificantly influenced the wind speed and SLP-based intensities for hurricanes Katrina, Irma and Maria, suggesting the possibility that climate variability—rather than anthropogenic warming—may have driven the active 2005 and 2017 Atlantic hurricane seasons, which were indeed characterized by especially warm tropical Atlantic SSTs. However, climate change at the time of these hurricanes significantly enhanced rainfall by 4%–9% and increased the probability of extreme rainfall rates, suggesting that climate change to date has already begun to increase tropical cyclone rainfall. Investigation of additional tropical cyclones is needed before making a general conclusion.

We then considered how 15 tropical cyclone events sampled globally could change if similar events were to occur at the end of the twenty-first century under the RCP4.5, RCP6.0 and RCP8.5 scenarios. We found a substantial and significant future intensification in the majority (11 of 13) of intense tropical cyclone events, based on wind speed and SLP, consistent with maximum potential intensity theory. Analysis of SST and tropical tropopause temperature changes is planned to understand the physical mechanisms behind these responses. In addition, we found robust increases in future tropical cyclone rainfall, with some events exceeding what would be expected by Clausius–Clapeyron alone and some events demonstrating a spatial pattern with concentrated rainfall increases near the centre of the tropical cyclone and drying in the outer-tropical-cyclone radii. These future changes in tropical cyclone intensity and rainfall could exacerbate societal impacts associated with ocean wind-waves[45], storm surge, flooding, and forests and ecosystems[46]. Simulations with and without convective parameterization suggest that convective parameterization introduces minimal uncertainty into the sign of projected changes in tropical cyclone intensity and rainfall, supporting confidence in projections of tropical cyclone activity from models with both parameterized convection and tropical-cyclone-permitting resolution (less than 0.25°).

The detection and attribution of anthropogenic changes in tropical cyclone events is a rapidly emerging science and methodology[47], especially as supercomputing advances enable ensembles of convection-permitting simulations. Our use of a dynamical climate model allows us to perform controlled experiments that focus on specific events and include various complexities of relevant physical processes. One important physical process for tropical cyclones that is missing from our model design is atmosphere–ocean coupling. In reality, tropical cyclone winds typically induce a 'cold wake' of upper-ocean temperatures that can provide a negative feedback on tropical cyclone intensity, depending on the tropical cyclone's intensity and translation speed and the ocean heat content and salinity structure[40,48,49]. Therefore, lack of coupling in the model can lead to tropical cyclones that are more intense and frequent compared to slab–ocean and fully coupled atmosphere–ocean simulations[50,51]. The atmosphere-only simulations presented in this study may overestimate tropical cyclone intensity, and additional research would help to quantify this uncertainty. In addition, because we used a single climate model, we have not examined model structural uncertainty, and results from other convection-permitting models could vary from those presented here.

Online content

Any methods, additional references, Nature Research reporting summaries, source data, statements of data availability and associated accession codes are available at https://doi.org/10.1038/s41586-018-0673-2.

Received: 15 April 2018; Accepted: 4 September 2018;
Published online 14 November 2018.

1. National Oceanic and Atmospheric Administration (NOAA) National Centers for Environmental Information (NCEI). *Billion-Dollar Weather and Climate Disasters* https://www.ncdc.noaa.gov/billions/ (NOAA NCEI, 2018).
2. Grossmann, I. & Morgan, M. G. Tropical cyclones, climate change, and scientific uncertainty: what do we know, what does it mean, and what should be done? *Clim. Change* **108**, 543–579 (2011).
3. Walsh, K. J. E. et al. Tropical cyclones and climate change. *WIREs Clim. Chang.* **7**, 65–89 (2016).
4. Sobel, A. H. et al. Human influence on tropical cyclone intensity. *Science* **353**, 242–246 (2016).
5. Landsea, C. W., Vecchi, G. A., Bengtsson, L. & Knutson, T. R. Impact of duration thresholds on Atlantic tropical cyclone counts. *J. Clim.* **23**, 2508–2519 (2010).
6. Landsea, C. W., Harper, B. A., Hoarau, K. & Knaff, J. A. Can we detect trends in extreme tropical cyclones? *Science* **313**, 452–454 (2006).
7. Vecchi, G. A. & Knutson, T. R. On estimates of historical north Atlantic tropical cyclone activity. *J. Clim.* **21**, 3580–3600 (2008).
8. Emanuel, K. Increasing destructiveness of tropical cyclones over the past 30 years. *Nature* **436**, 686–688 (2005).
9. Webster, P. J., Holland, G. J., Curry, J. A. & Chang, H. R. Changes in tropical cyclone number, duration, and intensity in a warming environment. *Science* **309**, 1844–1846 (2005).
10. Klotzbach, P. J. Trends in global tropical cyclone activity over the past twenty years (1986–2005). *Geophys. Res. Lett.* **33**, L10805 (2006).
11. Kossin, J. P., Knapp, K. R., Vimont, D. J., Murnane, R. J. & Harper, B. A. A globally consistent reanalysis of hurricane variability and trends. *Geophys. Res. Lett.* **34**, L04815 (2007).
12. Landsea, C. W., Pielke, R. A., Mestas-Nunez, A. & Knaff, J. A. Atlantic basin hurricanes: indices of climatic changes. *Clim. Change* **42**, 89–129 (1999).
13. Goldenberg, S. B., Landsea, C. W., Mestas-Nunez, A. M. & Gray, W. M. The recent increase in Atlantic hurricane activity: causes and implications. *Science* **293**, 474–479 (2001).
14. Gray, W. M. Atlantic seasonal hurricane frequency. 1. El-Nino and 30-mb quasi-biennial oscillation influences. *Mon. Weath. Rev.* **112**, 1649–1668 (1984).
15. Vimont, D. J. & Kossin, J. P. The Atlantic Meridional Mode and hurricane activity. *Geophys. Res. Lett.* **34**, L07709 (2007).
16. Patricola, C. M., Saravanan, R. & Chang, P. The impact of the El Nino-Southern Oscillation and Atlantic Meridional Mode on seasonal Atlantic tropical cyclone activity. *J. Clim.* **27**, 5311–5328 (2014).
17. Patricola, C. M., Chang, P. & Saravanan, R. Degree of simulated suppression of Atlantic tropical cyclones modulated by flavour of El Nino. *Nat. Geosci.* **9**, 155–160 (2016).
18. Gualdi, S., Scoccimarro, E. & Navarra, A. Changes in tropical cyclone activity due to global warming: results from a high-resolution coupled general circulation model. *J. Clim.* **21**, 5204–5228 (2008).
19. Knutson, T. R., Sirutis, J. J., Garner, S. T., Vecchi, G. A. & Held, I. M. Simulated reduction in Atlantic hurricane frequency under twenty-first-century warming conditions. *Nat. Geosci.* **1**, 359–364 (2008).
20. Knutson, T. R. et al. Tropical cyclones and climate change. *Nat. Geosci.* **3**, 157–163 (2010).
21. Wehner, M. et al. Resolution dependence of future tropical cyclone projections of CAM5.1 in the US CLIVAR Hurricane Working Group idealized configurations. *J. Clim.* **28**, 3905–3925 (2015).
22. Wehner, M. F., Reed, K. A., Loring, B., Stone, D. & Krishnan, H. Changes in tropical cyclones under stabilized 1.5 °C and 2.0 °C global warming scenarios as simulated by the Community Atmospheric Model under the HAPPI protocols. *Earth Syst. Dyn.* **9**, 187–195 (2018).
23. Emanuel, K. A. Downscaling CMIP5 climate models shows increased tropical cyclone activity over the 21st century. *Proc. Natl Acad. Sci. USA* **110**, 12219–12224 (2013).
24. Emanuel, K. A. The dependence of hurricane intensity on climate. *Nature* **326**, 483–485 (1987).
25. Knutson, T. R. & Tuleya, R. E. Impact of CO_2-induced warming on simulated hurricane intensity and precipitation: sensitivity to the choice of climate model and convective parameterization. *J. Clim.* **17**, 3477–3495 (2004).
26. Bender, M. A. et al. Modeled impact of anthropogenic warming on the frequency of intense Atlantic hurricanes. *Science* **327**, 454–458 (2010).
27. Hill, K. A. & Lackmann, G. M. The impact of future climate change on TC intensity and structure: a downscaling approach. *J. Clim.* **24**, 4644–4661 (2011).
28. Knutson, T. R. et al. Dynamical downscaling projections of twenty-first-century Atlantic hurricane activity: CMIP3 and CMIP5 model-based scenarios. *J. Clim.* **26**, 6591–6617 (2013).
29. Walsh, K. J. E. et al. Hurricanes and climate: the U.S. CLIVAR Working Group on hurricanes. *Bull. Am. Meteorol. Soc.* **96**, 997–1017 (2015).
30. Villarini, G. et al. Sensitivity of tropical cyclone rainfall to idealized global-scale forcings. *J. Clim.* **27**, 4622–4641 (2014).
31. Scoccimarro, E. et al. Intense precipitation events associated with landfalling tropical cyclones in response to a warmer climate and increased CO_2. *J. Clim.* **27**, 4642–4654 (2014).

32. Wright, D. B., Knutson, T. R. & Smith, J. A. Regional climate model projections of rainfall from US landfalling tropical cyclones. *Clim. Dyn.* **45**, 3365–3379 (2015).
33. Scoccimarro, E. et al. in *Hurricanes and Climate Change* (eds Collins, J. & Walsh, K.) 243–255 (Springer, Cham, 2017).
34. Allen, M. R. & Ingram, W. J. Constraints on future changes in climate and the hydrologic cycle. *Nature* **419**, 224–232 (2002).
35. Risser, M. D. & Wehner, M. F. Attributable human-induced changes in the likelihood and magnitude of the observed extreme precipitation during hurricane Harvey. *Geophys. Res. Lett.* **44**, 12457–12464 (2017).
36. van Oldenborgh, G. J. et al. Attribution of extreme rainfall from hurricane Harvey, August 2017. *Environ. Res. Lett.* **12**, 124009 (2017).
37. Wang, S. Y. et al. Quantitative attribution of climate effects on hurricane Harvey's extreme rainfall in Texas. *Environ. Res. Lett.* **13**, 054014 (2018).
38. Emanuel, K. Assessing the present and future probability of hurricane Harvey's rainfall. *Proc. Natl Acad. Sci. USA* **114**, 12681–12684 (2017).
39. Gray, W. M. Global view of origin of tropical disturbances and storms. *Mon. Weath. Rev.* **96**, 669–700 (1968).
40. Huang, P., Lin, I. I., Chou, C. & Huang, R. H. Change in ocean subsurface environment to suppress tropical cyclone intensification under global warming. *Nat. Commun.* **6**, 7188 (2015).
41. Emanuel, K., Solomon, S., Folini, D., Davis, S. & Cagnazzo, C. Influence of tropical tropopause layer cooling on Atlantic hurricane activity. *J. Clim.* **26**, 2288–2301 (2013).
42. Wing, A. A., Emanuel, K. & Solomon, S. On the factors affecting trends and variability in tropical cyclone potential intensity. *Geophys. Res. Lett.* **42**, 8669–8677 (2015).
43. Vecchi, G. A. & Soden, B. J. Increased tropical Atlantic wind shear in model projections of global warming. *Geophys. Res. Lett.* **34**, L08702 (2007).
44. Kaplan, J. et al. *Improvement in the Rapid Intensity Index by Incorporation of Inner-core Information*. JHT final report. https://www.nhc.noaa.gov/jht/09-11reports/final_Kaplan_JHT11.pdf (NOAA, 2011).
45. Timmermans, B., Patricola, C. M. & Wehner, M. F. Simulation and analysis of hurricane-driven extreme wave climate under two ocean warming scenarios. *Oceanography* **31**, https://doi.org/10.5670/oceanog.2018.218 (2018).
46. Feng, Y. et al. Rapid remote sensing assessment of impacts from hurricane Maria on forests of Puerto Rico. Preprint at https://peerj.com/preprints/26597/ (2018).
47. Wehner, M. F., Zarzycki, C. & Patricola, C. M. in *Hurricane Risk* (eds Collins, J. & Walsh, K.) Ch. 12 (Springer, Cham, in the press).
48. Lin, I. I., Pun, I. F. & Wu, C. C. Upper-ocean thermal structure and the western north Pacific category 5 typhoons. Part II: dependence on translation speed. *Mon. Weath. Rev.* **137**, 3744–3757 (2009).
49. Balaguru, K. et al. Ocean barrier layers' effect on tropical cyclone intensification. *Proc. Natl Acad. Sci. USA* **109**, 14343–14347 (2012).
50. Zarzycki, C. M. Tropical cyclone intensity errors associated with lack of two-way ocean coupling in high-resolution global simulations. *J. Clim.* **29**, 8589–8610 (2016).
51. Li, H. & Sriver, R. L. Tropical cyclone activity in the high-resolution community earth system model and the impact of ocean coupling. *J. Adv. Model. Earth Syst.* **10**, 165–186 (2018).

Acknowledgements This material is based on work supported by the US Department of Energy, Office of Science, Office of Biological and Environmental Research, Climate and Environmental Sciences Division, Regional and Global Climate Modeling Program, under award number DE-AC02-05CH11231. This research used resources of the National Energy Research Scientific Computing Center, a DOE Office of Science User Facility supported by the Office of Science of the US Department of Energy under contract number DE-AC02-05CH11231. We thank H. Krishnan for setting up access to the simulation data at NERSC.

Reviewer information *Nature* thanks J. Manganello and the other anonymous reviewer(s) for their contribution to the peer review of this work.

Author contributions C.M.P. and M.F.W. conceived the project and developed the methodology. C.M.P. performed the simulations, with climate perturbations from M.F.W., and analysed the data. C.M.P. wrote the manuscript with contributions from M.F.W.

Competing interests The authors declare no competing interests.

Additional information
Extended data is available for this paper at https://doi.org/10.1038/s41586-018-0673-2.

Correspondence and requests for materials should be addressed to C.M.P.

METHODS

We performed hindcast simulations with the Weather Research and Forecasting (WRF) regional climate model[52] version 3.8.1, which is developed by the National Center for Atmospheric Research (NCAR). The regional model is well suited for this study for several reasons. First, the use of lateral boundary conditions (LBCs) allows us to prescribe a tighter constraint on the large-scale circulation (that is, steering flow) of the tropical cyclone hindcast than if a global model were used. This is beneficial because it is necessary for the hindcasts to reproduce observed tropical cyclone tracks well, given that tropical cyclone characteristics such as intensity and rainfall are sensitive to underlying SST and surrounding environmental conditions. In addition, such 'well behaved' tracks among different climate scenarios enables a 'fair' comparison of the tropical cyclone responses. That is, a simulated tropical cyclone that deviates substantially from the observed track does not truly represent that tropical cyclone. (We typically used a criterion of about 3° of latitude or longitude, with some subjective judgement.) Second, whereas global climate models typically use the hydrostatic approximation to simplify the vertical momentum equation, WRF is non-hydrostatic and therefore more appropriate for simulating small-scale convective processes. Finally, the regional domain allows us to perform ensembles of simulations at convection-permitting resolution, which would be computationally less feasible with a global model.

The control simulations consist of hindcasts representing 15 tropical cyclone events (Fig. 1 and Extended Data Table 1) in the historical conditions in which they actually occurred. We selected tropical cyclones that were particularly impactful and represent various tropical cyclone basins. The North Indian Ocean was omitted owing to model instability probably associated with the Tibetan Plateau, and hurricane Harvey was omitted owing to poor hindcast skill. Initial conditions and LBCs for the historical hindcast simulations were taken from the six-hourly National Centers for Environmental Prediction (NCEP) Climate Forecast System (CFS) Reanalysis[53] for all tropical cyclones occurring before March 2011, and from the NCEP Climate Forecast System Version 2 (ref. [54]) for tropical cyclones occurring in March 2011 or later. No adjustments or data assimilation were performed on the initial conditions or LBCs. Model initialization time (Extended Data Table 1) was chosen to represent the tropical cyclone for as much of its lifetime as possible, while still being able to realistically simulate the observed track, since an earlier initialization time generally produced larger deviations between the observed and simulated tropical cyclone track. The tropical cyclone intensity within the model adjusts from its initial condition within hours. We did not test whether the simulated anthropogenic influence on tropical cyclones is sensitive to initialization time. SST was prescribed from the daily 0.25° National Oceanic and Atmospheric Administration Optimum Interpolation (NOAA-OI) dataset[55] for all tropical cyclones, except hurricanes Irma and Maria, which used the NCEP Climate Forecast System Version 2. Greenhouse gas concentrations, including CO_2, CH_4, N_2O, CFC-11, CFC-12 and CCl_4, were prescribed according to refs [56,57]. A ten-member ensemble of each simulation was generated using the Stochastic Kinetic Energy Backscatter Scheme (SKEBS)[58], which represents uncertainty from interactions with unresolved scales by introducing temporally and spatially correlated perturbations to the rotational wind components and potential temperature. The SST, initial condition and LBCs are identical for each ensemble member within a simulation set.

We also performed experiments representing hurricanes Katrina, Irma and Maria if they were to occur in a pre-industrial climate and all 15 tropical cyclone events at the end of the twenty-first century under the RCP4.5, RCP6.0 and RCP8.5 emissions scenarios, as permitted by supercomputing resources. SSTs, initial conditions and LBCs for the pre-industrial and Representative Concentration Pathway experiments were based on those from the historical simulations, with adjustments to remove and add, respectively, the thermodynamic component of anthropogenic climate change, using the 'pseudo-global warming' approach detailed in refs [47,59]. In the pseudo-global warming experiments, the model's boundary conditions use the same input data as in the control simulations for the historical period, but with a climate change signal added. This methodology has been used to study anthropogenic influences on individual tropical cyclone events at similar horizontal resolutions used in this study[60–65]. The novelty here is in investigating over a dozen tropical cyclone cases under multiple emissions scenarios at such a resolution. The variables adjusted in the LBCs include temperature, relative humidity and geopotential height. We did not adjust horizontal winds in the LBCs to minimize possible perturbations to the simulated hurricane track, although tests on a subset of simulations showed that the response in tropical cyclone intensity to anthropogenic forcing is insensitive to whether circulation changes were applied to the LBCs. The experimental design, therefore, prescribes no changes in large-scale vertical wind shear. We note that any potential changes in vertical wind shear[43] may be expected to change the summary statistics of tropical cyclone activity (for example, average annual number of tropical cyclones). However, even given average changes in wind shear, it is conceivable that individual tropical cyclone events may occur under shear conditions similar to those of the present climate, especially since some climate models project relatively weak shear changes in the Atlantic and Pacific basins[66]. Therefore, by prescribing zero change in horizontal winds in the climate change simulations, the large-scale vertical shear state is included in the conditionality of the 'worst-case-scenario' tropical cyclone event occurrence. This allows us to evaluate changes in tropical cyclone magnitudes given similar shear conditions, which may become more or less likely in changing climates.

The variables adjusted in the initial conditions include surface temperature (land and sea), 2-m air temperature, 2-m specific humidity, SLP and surface pressure. Greenhouse gas concentrations were modified in the WRF climate model according to refs [56,57,67]. The experimental design is similar to the hindcast methodology used to understand anthropogenic contributions to the extreme flood event that affected the Boulder, Colorado, region in September 2013[68].

Anthropogenic climate change from the pre-industrial to historical period was estimated using Community Atmosphere Model (CAM) simulations from the Climate of the 20th Century Plus Detection and Attribution (C20C+ D&A) Project[69] (D. A. Stone et al., submitted manuscript). The 'factual' C20C+ simulation consists of a 50-member ensemble of 1° resolution CAM5.1 integrations forced with historical radiative and land-surface boundary conditions and SST, and the 'counterfactual' simulation uses radiative forcing from the year 1855, with SST and sea ice modified using perturbations from coupled atmosphere–ocean simulations of the Coupled Model Intercomparison Project Phase 5 (CMIP5; D. A. Stone & P. Pall, submitted manuscript). The climate change perturbation for the pre-industrial hurricane Katrina experiment was calculated as the difference between the factual and the counterfactual C20C+ simulations for August 2005; this perturbation was then subtracted from the historical boundary conditions. For hurricanes Irma and Maria, the perturbation was estimated as the difference between the September 1996–2016 climatology of the factual minus counterfactual C20C+ simulations, as the C20C+ simulations did not extend to 2017 at the time of this study.

Anthropogenic climate change for the end of the twenty-first century was based on simulations from the Community Climate System Model (CCSM4) of the CMIP5. The climate change perturbation for the RCP8.5 hurricane Katrina experiment was calculated as the 2081–2100 August climatology from the CCSM4 RCP8.5 simulation minus the 1980–2000 August climatology from the CCSM4 historical simulation. This perturbation was then added to the historical boundary conditions. The perturbations for all other tropical cyclones were calculated in the same way, but for the month in which the tropical cyclone occurred (for example, September for hurricanes Irma and Maria).

By using one global model to provide climate change perturbations, the results here apply for the climate sensitivity characteristic of that model. The uncertainty due to the range of climate sensitivities among different models was not accounted for, in favour of using supercomputing resources towards 15 tropical cyclone events, convection-permitting resolution, ten-member ensembles and multiple Representative Concentration Pathway scenarios. We note that the climate sensitivity of the CCSM4 model is among the lower of the coupled atmosphere–ocean global climate models of CMIP5[70,71], suggesting that the estimates of future change provided by this study may be conservative. The SST forcings for the CAM simulations from the C20C+ D&A Project were based on the multi-model mean of the CMIP5, suggesting that the estimates of climate change influences from pre-industrial to present are near the centre of the range of models.

Simulations of all tropical cyclone events were performed at a convection-permitting horizontal resolution of 4.5 km, with 44 levels in the vertical and a model top at 20 hPa. To investigate uncertainty in the response of tropical cyclones to anthropogenic forcings due to convective parameterization, we performed additional simulations of hurricane Katrina at horizontal resolutions of 3 km without parameterization, 9 km both without and with parameterization (Kain–Fritsch), and 27 km with parameterization, with 35 levels in the vertical and a model top at 50 hPa. The results are insensitive to vertical resolution and model top choices.

Simulated tropical cyclone coordinates are defined using the location of minimum SLP. Simulated three-hourly instantaneous maximum 10-m tropical cyclone wind speeds are compared with the observed six-hourly maximum 1-min average sustained 10-m wind speed from the Revised Hurricane Database (HURDAT2[72,73]) and the Joint Typhoon Warning Center (JTWC) dataset as archived in the International Best Track Archive for Climate Stewardship (IBTrACS[74]) v03r10 database. Such differences in maximum wind speed definitions generate uncertainty in comparisons between observations and model simulations, and it is unclear whether there is a tendency for one definition to be systematically biased in a particular direction. The historical simulations appear to produce tropical cyclones with slightly weaker intensities than observed (Fig. 1), which may be related to these differences in intensity definitions between the model and observations, or to model limitations in horizontal resolution and/or physical approximations. Despite this uncertainty, the simulations with convection-permitting resolution perform substantially better in reproducing the approximate tropical cyclone intensities than simulations with convective parameterization (Fig. 3d). In addition, we acknowledge that while climate models are imperfect, the robust climate change response for hurricane Katrina at horizontal resolutions between

3 km and 27 km provides support for the contention that 4.5-km resolution is sufficient to capture the influence of climate change on tropical cyclones in the full set of experiments.

Code availability. Code for the WRF model, version 3.8.1, is available at http://www2.mmm.ucar.edu/wrf/users/downloads.html. Analytical scripts are available from the corresponding author on request.

Data availability

Simulation data are available at the National Energy Research Scientific Computing Center (NERSC) at http://portal.nersc.gov/cascade/TC/.

52. Skamarock, W. C. & Klemp, J. B. A time-split nonhydrostatic atmospheric model for weather research and forecasting applications. *J. Comput. Phys.* **227**, 3465–3485 (2008).
53. Saha, S. et al. The NCEP Climate Forecast System Reanalysis. *Bull. Am. Meteorol. Soc.* **91**, 1015–1058 (2010).
54. Saha, S. et al. The NCEP Climate Forecast System Version 2. *J. Clim.* **27**, 2185–2208 (2014).
55. Reynolds, R. W. et al. Daily high-resolution-blended analyses for sea surface temperature. *J. Clim.* **20**, 5473–5496 (2007).
56. Tsutsumi, Y., Mori, K., Hirahara, T., Ikegami, M. & Conway, T. J. *Technical Report of Global Analysis Method for Major Greenhouse Gases by the World Data Center for Greenhouse Gases*. GAW Report No. 184, https://www.wmo.int/pages/prog/arep/gaw/documents/TD_1473_GAW184_web.pdf (World Meteorological Organization, 2009).
57. Bullister, J. L. *Atmospheric Histories (1765-2015) for CFC-11, CFC-12, CFC-113, CCl4, SF6 and N2O. NDP-095*. http://cdiac.ess-dive.lbl.gov/ftp/oceans/CFC_ATM_Hist/CFC_ATM_Hist_2015/ (Carbon Dioxide Information Analysis Center, Oak Ridge National Laboratory, US Department of Energy, 2015).
58. Shutts, G. A kinetic energy backscatter algorithm for use in ensemble prediction systems. *Q. J. R. Meteorol. Soc.* **131**, 3079–3102 (2005).
59. Schär, C., Frei, C., Lüthi, D. & Davies, H. C. Surrogate climate-change scenarios for regional climate models. *Geophys. Res. Lett.* **23**, 669–672 (1996).
60. Takayabu, I. et al. Climate change effects on the worst-case storm surge: a case study of typhoon Haiyan. *Environ. Res. Lett.* **10**, 064011 (2015).
61. Lackmann, G. M. Hurricane Sandy before 1900 and after 2100. *Bull. Am. Meteorol. Soc.* **96**, 547–560 (2015).
62. Ito, R., Takemi, T. & Arakawa, O. A possible reduction in the severity of typhoon wind in the northern part of Japan under global warming: a case study. *Sci. Online Lett. Atmos.* **12**, 100–105 (2016).
63. Nakamura, R., Shibayama, T., Esteban, M. & Iwamoto, T. Future typhoon and storm surges under different global warming scenarios: case study of typhoon Haiyan (2013). *Natural Hazards* **82**, 1645–1681 (2016).
64. Takemi, T., Ito, R. & Arakawa, O. Effects of global warming on the impacts of Typhoon Mireille (1991) in the Kyushu and Tohoku regions. *Hydrol. Res. Lett.* **10**, 81–87 (2016).
65. Kanada, S. et al. A multimodel intercomparison of an intense typhoon in future, warmer climates by four 5-km-mesh models. *J. Clim.* **30**, 6017–6036 (2017).
66. Wehner, M. F. et al. Towards direct simulation of future tropical cyclone statistics in a high-resolution global atmospheric model. *Adv. Meteorol.* **2010**, 915303 (2010).
67. Meinshausen, M. et al. The RCP greenhouse gas concentrations and their extensions from 1765 to 2300. *Clim. Change* **109**, 213–241 (2011).
68. Pall, P. et al. Diagnosing conditional anthropogenic contributions to heavy Colorado rainfall in September 2013. *Weather Clim. Extrem.* **17**, 1–6 (2017).
69. Stone, D. A. et al. A basis set for exploration of sensitivity to prescribed ocean conditions for estimating human contributions to extreme weather in CAM5.1-1degree. *Weather Clim. Extrem.* **19**, 10–19 (2018).
70. Vial, J., Dufresne, J.-L. & Bony, S. On the interpretation of inter-model spread in CMIP5 climate sensitivity estimates. *Clim. Dyn.* **41**, 3339–3362 (2013).
71. Andrews, T., Gregory, J. M., Webb, M. J. & Taylor, K. E. Forcing, feedbacks and climate sensitivity in CMIP5 coupled atmosphere-ocean climate models. *Geophys. Res. Lett.* **39**, L09712 (2012).
72. Landsea, C. W. et al. in *Hurricanes and Typhoons: Past, Present and Future* (eds Murnane, R. J. & Liu, K.-B.) 177–221 (Columbia Univ. Press, New York, 2004).
73. Landsea, C. W. & Franklin, J. L. Atlantic hurricane database uncertainty and presentation of a new database format. *Mon. Weath. Rev.* **141**, 3576–3592 (2013).
74. Knapp, K. R., Kruk, M. C., Levinson, D. H., Diamond, H. J. & Neumann, C. J. The International Best Track Archive for Climate Stewardship (IBTrACS): unifying tropical cyclone best track data. *Bull. Am. Meteorol. Soc.* **91**, 363–376 (2010).

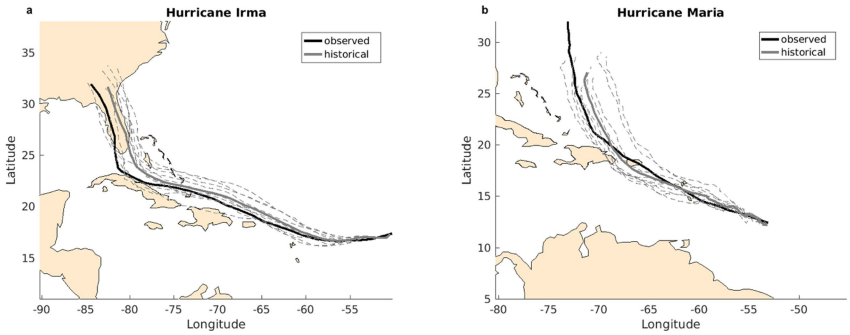

Extended Data Fig. 1 | Tropical cyclone tracks. a, **b**, The observed hurricane track (black) with simulated tropical cyclone tracks from ten ensemble members (grey dashed lines) and the ensemble mean (grey solid line) of the historical simulation for hurricanes Irma (**a**) and Maria (**b**) at 4.5-km resolution.

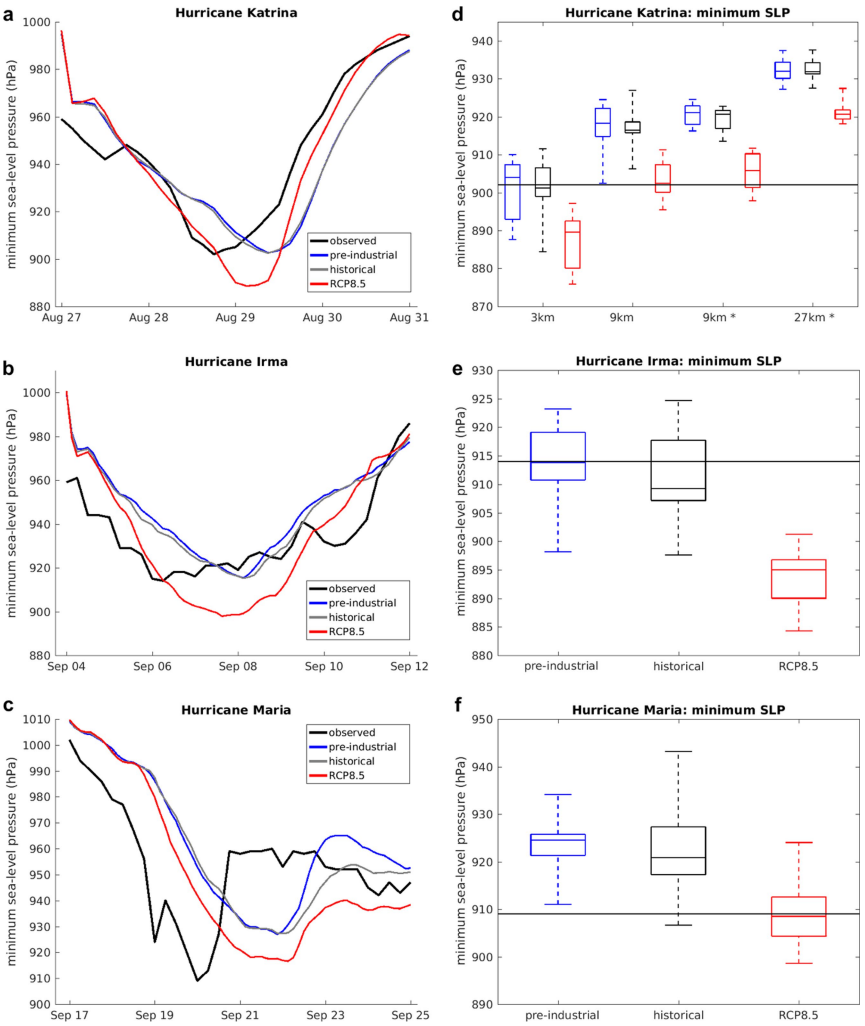

Extended Data Fig. 2 | Time series and boxplots of tropical cyclone minimum SLP. a–c, The time series of minimum SLP (hPa) from observations (black) and the ensemble mean of the pre-industrial (blue), historical (grey) and RCP8.5 (red) simulations of hurricane Katrina at 3-km resolution (**a**) and hurricanes Irma (**b**) and Maria (**c**) at 4.5-km resolution. **d–f**, Boxplots of minimum SLP (hPa) from the ten-member ensemble of pre-industrial (blue), historical (black) and RCP8.5 (red) simulations of hurricane Katrina at 3-km, 9-km and 27-km resolution (**d**), and of hurricanes Irma (**e**) and Maria (**f**) at 4.5-km resolution. The centre line denotes the median, box limits denote lower and upper quartiles, and whiskers denote the minimum and maximum. The observed minimum SLP is marked with a horizontal black line. Simulations that used convective parameterization are denoted by asterisks.

Basin	TC	resolution	hist.-preind.	RCP4.5-hist.	RCP6.0-hist.	RCP8.5-hist.	historical	observed
Atlantic	Katrina	27 km (P)	0.2			-11.2 **	932	902
		9 km (P)	-1.2			-14.0 **	920	902
		9 km	0.6			-13.8 **	917	902
		3 km	-0.2			-13.8 **	901	902
		4.5 km		-7.7 **	-7.6 **	-8.7 **	905	902
	Irma		1.3	-11.4 **	-13.7 **	-17.5 **	912	914
	Maria		1.0	-8.0 **	-12.6 **	-13.8 **	923	909
	Andrew			6.0	6.1	7.0 *	948	922
	Bob			3.1 **	1.7 **	7.8 **	979	950
	Floyd			-12.3 **	-14.9 **		928	921
	Gilbert			-17.6 **	-15.2 **	-20.8 **	940	888
	Ike			-15.2 **	-17.6 **	-21.7 **	932	935
	Matthew			-12.5 **	-12.8 **	-17.0 **	934	934
Eastern Pacific	Iniki			3.2	6.2	-7.2 **	949	938
NW Pacific	Haiyan			-12.0 **	-11.9 **	-20.6 **	926	895
	Morakot			-0.1			976	945
	Songda			-12.1 **	-4.7 **		940	925
South Pacific	Yasi			-9.9 **	-11.7 **	-17.7 **	957	929
SW Indian	Gafilo			-15.4 **	-12.5 **	-24.6 **	948	895

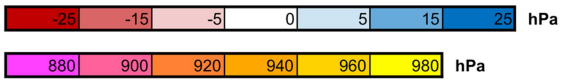

Extended Data Fig. 3 | Tropical cyclone minimum SLP. Heatmaps are shown of the ensemble-mean difference in minimum SLP (in hPa) between the historical and pre-industrial simulations and between the RCP4.5, RCP6.0 and RCP8.5 simulations and the historical simulation (blue/red), with minimum SLP from observations and the ensemble-mean historical simulation (yellow/magenta). Light grey denotes substantial differences between the simulated and the observed tropical cyclone tracks and dark grey denotes simulations that were not performed. *Changes significant at the 10% level; **changes significant at the 5% level. Simulations that used convective parameterization are denoted 'P'.

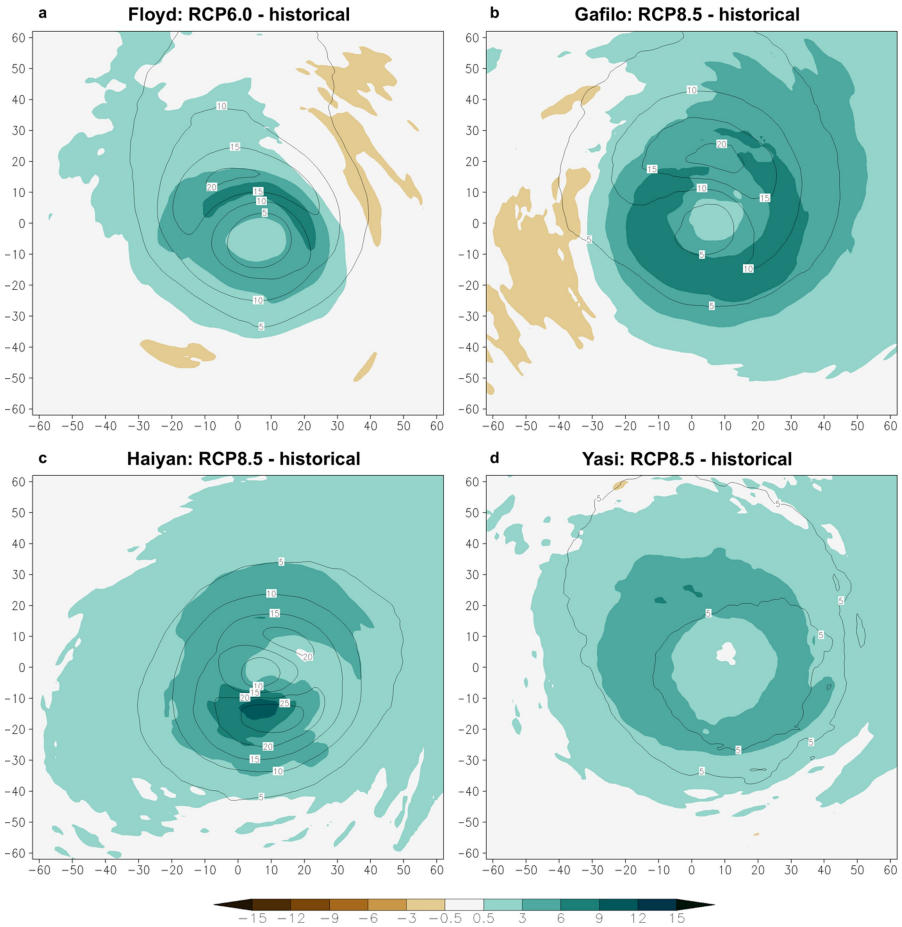

Extended Data Fig. 4 | Tropical cyclone rainfall composites. **a**–**d**, Rainfall rate (colour scale, in millimetres per hour) relative to the tropical cyclone centre and throughout the simulated tropical cyclone lifetime from the ensemble mean of the RCP6.0 minus historical simulation of hurricane Floyd (**a**) and the RCP8.5 minus historical simulation of cyclone Gafilo (**b**), typhoon Haiyan (**c**) and cyclone Yasi (**d**) at 4.5-km resolution. Contours denote the rainfall rate (in millimetres per hour) from the corresponding historical simulation. The axes show the number of model grid points from the tropical cyclone centre.

Extended Data Table 1 | List of tropical cyclone events

Basin	TC	Historical simulation period
Atlantic	Katrina	27 – 31 Aug, 2005
	Irma	4 – 13 Sep, 2017
	Maria	17 – 25 Sep, 2017
	Andrew	23 – 28 Aug, 1992
	Bob	18 – 21 Aug, 1991
	Floyd	13 – 18 Sep, 1999
	Gilbert	13 – 19 Sep, 1988
	Ike	6 – 15 Sep, 2008
	Matthew	1 – 7 Oct, 2016
East Pacific	Iniki	8 – 14 Sep, 1992
North West Pacific	Haiyan	5 – 11 Nov, 2013
	Morakot	6 – 12 Aug, 2009
	Songda	3 – 9 Sep, 2004
South Pacific	Yasi	31 Jan – 5 Feb, 2011
South West Indian	Gafilo	4 – 10 Mar, 2004

List of tropical cyclone events considered in this study, with simulation period. All initial conditions are at time 00z (midnight UTC).